AIAA JOURNAL
Vol. 30, No. 3, March 1992

Approximate Solutions for Oblique Detonations in the Hypersonic Limit

Joseph M. Powers*
University of Notre Dame, Notre Dame, Indiana 46556
and
D. Scott Stewart†
University of Illinois at Urbana-Champaign, Urbana, Illinois 61801

This article describes analytic solutions for hypersonic flow of a premixed reactive ideal gas over a wedge. The flow is characterized by a shock followed by a spatially resolved reaction zone. Explicit solutions are given for the irrotational flowfield behind a straight shock attached to a curved wedge and for the rotational flowfield behind a curved shock attached to a straight wedge. Continuous solution trajectories exist that connect the state just past the shock to the equilibrium end states found from a Rankine-Hugoniot theory for changes across oblique discontinuities with energy release. The analytic results are made possible by the hypersonic approximation, which implies that a fluid particle's kinetic energy is much larger than its thermal and chemical energy. The leading order solution is an inert oblique shock. The effects of heat release are corrected for at the next order. These results can be used to verify numerical results and are necessary for more advanced analytic studies. In addition, the theory has application to devices such as the oblique detonation wave engine, the ram accelerator, hypersonic airframes, or re-entry vehicles.

Introduction

RENEWED interest in hypersonic propulsion has spurred research involving oblique detonation waves. The two-dimensional structure of steady reactive flow over a wedge, as sketched in Fig. 1, is considered here. A uniform supersonic upstream flow encounters a wedge, inclined at angle θ, producing an oblique shock, inclined at angle β, which initiates a chemical reaction that takes place over a finite region. We call such a structure an oblique detonation.

Among the devices where oblique detonations are a relevant concern are the oblique detonation wave engine (ODWE). The ODWE utilizes a wedge to generate a shock wave and subsequent combustion in a premixed fuel-air mixture. The study of Pratt et al.[1] of oblique detonation discontinuities, which led us to consider this problem, gives a fuller discussion of the ODWE. The ODWE and related re-entry and nonequilibrium flow problems motivated many early experimental, analytic, and numerical studies,[2-13] and also more recent, primarily numerical studies.[14-22] The ram accelerator[23] is another device that may be associated with oblique detonations.

Theoretical studies of oblique detonations have been of four types: Rankine-Hugoniot analyses,[1,2,9,19] perturbation analyses,[3,7,12] numerical analyses based on the method of characteristics,[8,13,22] and unsteady numerical analyses.[14-18,20-22] Rankine-Hugoniot analyses, such as those performed by Siestrunck et al.,[2] Gross,[9] and, more recently, Pratt et al.[1] and Buckmaster and Lee,[19] assume that heat is released in an infinitely thin zone coincident with the oblique shock. In assuming that the heat is released instantaneously, jump equations with heat release are formed, and an algebraic solution for the reacted state is obtained. The analysis presumes that a structure linking the shock state to an equilibrium end state exists.

Perturbation methods can be used to describe this structure. Similar studies have considered vibrational relaxation of hypersonic flow over wedges with small angle (cf. Moore and Gibson[3] or Vincenti[7]) and $\mathcal{O}(1)$ angle (Lee[12]). In a related study, Clarke[4] considered flow slightly turned by an expansion corner. Other related studies concern shock initiation of explosives. In these studies, a moving piston generates a shock, which ignites the explosive. There is a direct analog between one-dimensional, unsteady flow and two-dimensional, steady flow over small wedge angles; this has been called the hypersonic equivalence principle (cf. Anderson,[24] or for more background, Hayes and Probstein[25]). When the piston generates a strong overdriven shock, the effective heat release is small. Spence[6] and Fickett[26] carried out such an analysis using the ratio of chemical to kinetic energy as the perturbation parameter and obtained exact solutions. In fact, Fickett's paper led us to consider the perturbation scheme for the present study.

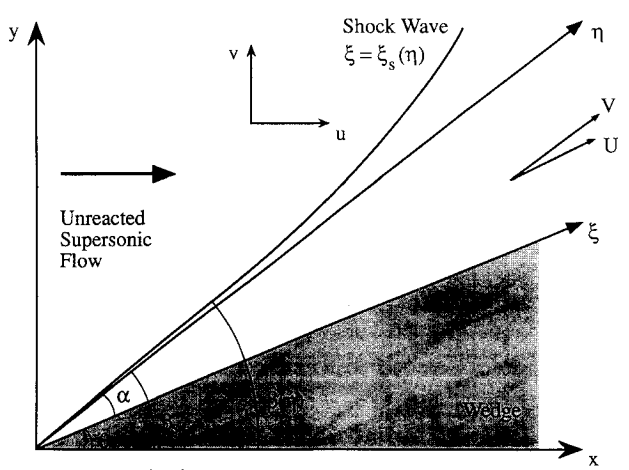

Fig. 1 Sketch of oblique detonation and coordinate axes.

Received Aug. 20, 1990; revision received March 22, 1991; accepted for publication March 26, 1991.

*Assistant Professor, Department of Aerospace and Mechanical Engineering. Member AIAA.

†Associate Professor, National Center for Supercomputing Applications and Department of Theoretical and Applied Mechanics, 104 S. Wright.

Numerical solutions for nonequilibrium flow over a wedge based on the method of characteristics have been performed by Capiaux and Washington,[8] Spurk et al.,[13] and Pandolfi et al.[22] This method can describe flow over a wedge or cone[10] with large deflection, flow with simultaneous chemical reactions, and large energy of reaction and is limited to supersonic postshock flows. Full unsteady numerical analyses of oblique detonations have been performed by Fujiwara et al.,[15] Wang et al.,[16] Bogdanoff and Brackett,[14] Cambier et al.,[17,18] Yungster,[20] and Yungster et al.[21] In addition to the basic oblique detonation phenomena, these studies variously consider the effects of many simultaneous reactions, viscosity, and dissociation.

In this article, we consider the configuration of Fig. 1 for an idealized system that retains enough features to describe an oblique detonation. The solution is not restricted to small wedge angles. Our goal is to describe the shape of an inert shock and the trailing two-dimensional reactive flowfield in terms of the initial flow properties, kinetic rate, and wall geometry and to demonstrate that the complete reaction state predicted by the detailed structure analysis can, in certain cases, be predicted by a reactive Rankine-Hugoniot analysis. Two cases are studied. The first has a straight shock attached to a curved wall. The second has a curved shock attached to a straight wall. Explicit solutions to the former have not appeared to our knowledge, though Anderson[24] and Shepherd[27] discuss this case. The latter is the exothermic analog to the case discussed by Lee for endothermic vibrational relaxation. It is shown in the curved-shock straight-wall case that the shock curvature approaches zero far from the wedge tip, in which case the simple straight shock solution adequately describes the flowfield.

Model Equations

The flow is modeled by the steady two-dimensional planar reactive Euler equations along with constitutive and shock jump equations. Dissociation, vibrational relaxation, or other real gas effects are not considered. It is assumed the fuel and oxidizer are premixed and can be treated as a single calorically perfect ideal gas. A one-step Arrhenius kinetic model is used. The results are valid in the limit in which both the heat of reaction and thermal energy of a fluid particle are small relative to its kinetic energy. An $\mathcal{O}(\varepsilon)$ correction to the constant shocked state is found using the reciprocal of the incoming Mach number squared as a perturbation parameter.

The following scales are used for this problem. Here, the o subscript indicates a preshock dimensional ambient condition and the * subscript indicates a dimensional variable:

$$\rho = \frac{\rho_*}{\rho_o}, \quad u = \frac{u_*}{M_o\sqrt{P_o/\rho_o}}, \quad v = \frac{v_*}{M_o\sqrt{P_o/\rho_o}}$$

$$P = \frac{P_*}{M_o^2 P_o}, \quad x = \frac{r_o x_*}{M_o\sqrt{P_o/\rho_o}}, \quad y = \frac{r_o y_*}{M_o\sqrt{P_o/\rho_o}} \tag{1}$$

The density, velocities, pressure, distances, and Mach number are ρ, u, v, P, x, y, and M, respectively. In the hypersonic limit, the length scale is defined by the reaction zone length when heat release has negligible influence. For $\mathcal{O}(1)$ dimensionless activation energy Θ, the length scale will be shown to be of the same order as the quotient of the freestream velocity $[u_o = M_o(\gamma P_o/\rho_o)^{1/2}]$ and the Arrhenius prefactor r_o. Here, γ is the ratio of specific heats. Density, velocity, and pressure scales have been chosen so that after the shock each is a $\mathcal{O}(1)$ quantity.

The dimensionless steady reactive Euler equations can be written as

$$\frac{\partial}{\partial x}(\rho u) + \frac{\partial}{\partial y}(\rho v) = 0 \tag{2a}$$

$$\rho\left(u\frac{\partial u}{\partial x} + v\frac{\partial u}{\partial y}\right) + \frac{\partial P}{\partial x} = 0 \tag{2b}$$

$$\rho\left(u\frac{\partial v}{\partial x} + v\frac{\partial v}{\partial y}\right) + \frac{\partial P}{\partial y} = 0 \tag{2c}$$

$$u\frac{\partial P}{\partial x} + v\frac{\partial P}{\partial y} - \gamma\frac{P}{\rho}\left(u\frac{\partial \rho}{\partial x} + v\frac{\partial \rho}{\partial y}\right) = \varepsilon(\gamma - 1)q\rho(1 - \lambda)e^{-\varepsilon\Theta\rho/P} \tag{2d}$$

$$u\frac{\partial \lambda}{\partial x} + v\frac{\partial \lambda}{\partial y} = (1 - \lambda)e^{-\varepsilon\Theta\rho/P} \tag{2e}$$

Equations (2a–c) describe conservation of mass and momenta. Equation (2d) is energy conservation written in a form that incorporates the assumption of an ideal gas and one-step Arrhenius kinetics. Equation (2e) is a rate law for Arrhenius kinetics with simple depletion. Here, λ is the mass fraction of the reaction product gas, $0 \le \lambda \le 1$, with $\lambda = 0$ and 1 corresponding to no reaction and complete reaction, respectively. Other dimensionless parameters are the heat of reaction $q = \rho_o q_o/P_o$, the activation energy $\Theta = E_o\rho_o/P_o$, and the perturbation parameter ε, defined to be the reciprocal of the square of the incoming Mach number, $\varepsilon = 1/M_o^2 = \gamma P_o/\rho_o u_o^2$. Here, q_o is the dimensional heat release and E_o the dimensional activation energy. The undisturbed flow properties are $\rho = 1$, $u = \gamma^{1/2}$, $v = 0$, $P = \varepsilon$, and $\lambda = 0$. The undisturbed flow approaches a shock inclined at an unknown angle β, located at y_s, assumed to be a function of x and attached to the wedge. The function $\beta(x)$ is chosen so that a downstream boundary condition of no mass flow through a wall located at $y = W(x)$ is satisfied. With s as a dummy integration variable, the shock location and downstream boundary condition are given by

$$y_s = \int_0^x \tan[\beta(s)]\,ds \tag{2f}$$

$$\frac{v}{u} = \frac{dW(x)}{dx} \qquad \text{on} \qquad y = W(x) \tag{2g}$$

Supplementary thermal and caloric state equations can be used to determine the internal energy e, temperature T, and frozen sound speed c: $P = \rho T$, $e = T/(\gamma - 1) - \varepsilon q\lambda$, $c^2 = \gamma P/\rho$. The vorticity ω_z and shock curvature κ are given by

$$\omega_z = \frac{\partial v}{\partial x} - \frac{\partial u}{\partial y} \tag{2h}$$

$$\kappa = \frac{d^2 y_s}{dx^2}\left[1 + \left(\frac{dy_s}{dx}\right)^2\right]^{-3/2} \tag{2i}$$

Rankine-Hugoniot Relations

Rankine-Hugoniot relations can be solved at each point in the reaction zone structure with the degree of heat release λq as a parameter. It is assumed here that the velocity tangent to the initial discontinuity remains constant through the discontinuity and at all points within the reaction zone. For a wave inclined at an angle β and the subscript 2 denoting the local state, the Rankine-Hugoniot relations are

$$\sqrt{\gamma}\sin\beta = \rho_2(u_2\sin\beta - v_2\cos\beta) \tag{3a}$$

$$\varepsilon + \gamma\sin^2\beta = P_2 + \rho_2(u_2\sin\beta - v_2\cos\beta)^2 \tag{3b}$$

$$\sqrt{\gamma}\cos\beta = u_2\cos\beta + v_2\sin\beta \tag{3c}$$

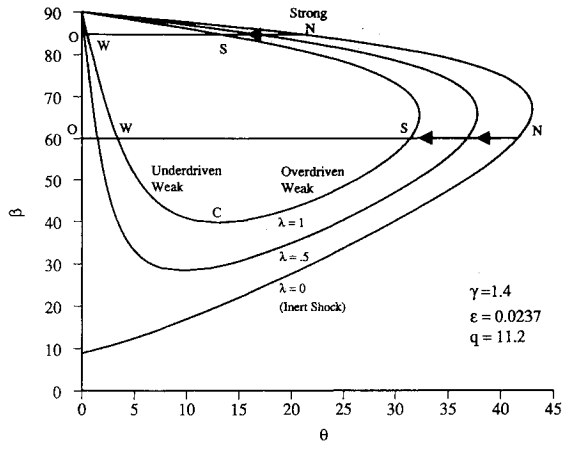

Fig. 2 Shock angle β vs wedge angle ($\lambda = 1$) or local flow angle ($0 \leq \lambda < 1$) from Rankine-Hugoniot analysis including path of chemical reaction for straight shock case.

$$\varepsilon\left(1 + \frac{\gamma - 1}{\gamma}\lambda q\right) + \frac{\gamma - 1}{2} = \frac{P_2}{\rho_2} + \frac{\gamma - 1}{2\gamma}(u_2^2 + v_2^2) \quad (3d)$$

The full solution for Eqs. (3a–d) in terms of β, γ, ε, and q is given in gasdynamics texts for the inert case ($\lambda = 0$) and by both Gross[9] and Pratt et al.[1] for the fully reacted ($\lambda = 1$) case. Some pertinent results are summarized, with Pratt et al.'s nomenclature adopted. For a wedge inclined at an angle θ, two physical solutions, strong and weak, can exist. Consistent with the inert oblique shock convention, the strong solution is taken to have the greater angle of inclination for a given wedge angle. It is likely that the appropriate branch is dictated by the nature of the downstream boundary conditions; however, the necessary analysis has not been performed to determine which boundary conditions are associated with which solution branch. Figure 2 shows the wave angle β as a function of the local flow angle, which for $\lambda = 1$ corresponds to the wedge angle θ. The exact solution of Eqs. (3a–d) is plotted here for $\gamma = 1.4$, $q = 11.2$, and $\lambda = 0$, 0.5, and 1. For $\lambda = 1$, the local minimum corresponds to a point where the Mach number in the direction normal to the wave M_n is sonic, analogous to a Chapman-Jouguet (CJ) detonation. For a given θ, complete reaction solutions on the weak branch with a final $M_n < 1$ are called overdriven weak oblique detonations, whereas those with a final $M_n > 1$ are called underdriven weak oblique detonations. When both velocity components are used to define a total Mach number, most of the weak branch is supersonic. In the hypersonic limit, it will be shown that the entire weak branch is supersonic.

There are many analogs between one-dimensional Zeldovich-von Neumann-Doering (ZND) detonation theory, described in detail by Fickett and Davis,[28] and oblique detonation theory. Unfortunately, inert oblique shock theory and ZND theory suggest two conflicting interpretations of the terms "strong" and "weak." The analogs in both the theory and nomenclature are described here. Strong and overdriven weak oblique detonation reaction paths for fixed shock angle β are sketched in Fig. 2. In both, the unreacted gas is shocked from O to N with no heat release within the infinitely thin shock. The shock induces exothermic reaction, giving rise to pressure, density, and velocity changes in the direction normal to the shock, whereas the velocity tangent to the shock remains constant through both the shock and reaction zone. The reaction proceeds to completion at S on a $\lambda = 1$ polar. From N to S, the local Mach number normal to the shock is subsonic. For a unique value of β, the reaction terminates at C, where the local Mach number normal to the shock is sonic. In this model with one-step irreversible kinetics, there is no path from the shocked state N to the underdriven weak point W. We speculate that with more complex models, such as those with competing exothermic and endothermic reactions, eigenvalue detonations could provide a path from N to W, which suggests that weak underdriven oblique detonations are possible. The families of partially reacted oblique detonation polars are analogous to partially reacted Hugoniot curves of ZND theory. The line of constant β is analogous to the Rayleigh line in ZND theory. The labels O, N, S, W, and C are those used by Fickett and Davis[28] for ZND detonations. In the adopted nomenclature, strong and overdriven weak solutions are analogous to ZND theory's strong solutions; underdriven weak solutions are analogous to ZND theory's weak solutions. This description is consistent with that of Anderson[24] and Shepherd.[27] As implied in these references, it is possible to construct an oblique detonation solution by forming a one-dimensional ZND solution, which, in general, must be obtained numerically, and adding a constant velocity component in the direction normal to the detonation. In subsequent sections, simple explicit overdriven weak and strong solutions will be constructed for the spatial distribution of all variables, requiring no numerical integration. These solutions will exhibit all of the features described here.

For our present purposes, we give a solution, parameterized by the product mass fraction λ, valid in the hypersonic limit. Though not illustrated in Fig. 2, it can be shown that in the hypersonic limit the complete reaction polar approaches the inert polar, the turning point C approaches the vertical axis, and that, near the origin, the inert polar approaches the curve $\theta = 2\beta/(\gamma + 1)$. In this limit, overdriven weak and strong solutions are available in a range $\mathcal{O}(\varepsilon) < \beta < \pi/2$. The asymptotic solution valid as $\varepsilon \to 0$ is

$$P_2 = \frac{2\gamma \sin^2\beta}{\gamma + 1} - \varepsilon\left[\frac{\gamma - 1}{\gamma + 1} + (\gamma - 1)\lambda q\right] \quad (4a)$$

$$\rho_2 = \frac{\gamma + 1}{\gamma - 1} - \varepsilon\left[\frac{2\gamma(\gamma + 1)}{(\gamma - 1)^2\gamma \sin^2\beta} + \frac{(\gamma + 1)^2\lambda q}{(\gamma - 1)\gamma \sin^2\beta}\right] \quad (4b)$$

$$\sqrt{u_2^2 + v_2^2} = \frac{\sqrt{\gamma}\sqrt{\gamma^2 + 2\gamma \cos 2\beta + 1}}{\gamma + 1} + \varepsilon\left[\frac{2\gamma(\gamma - 1) + (\gamma - 1)(\gamma^2 - 1)\lambda q}{\sqrt{\gamma}(\gamma + 1)\sqrt{\gamma^2 + 2\gamma \cos 2\beta + 1}}\right] \quad (4c)$$

$$\frac{v_2}{u_2} = \tan\theta = \frac{\sin 2\beta}{\gamma + \cos 2\beta} - \varepsilon\left[\frac{2\gamma(\gamma + 1)\cos\beta + \cos\beta(\gamma + 1)(\gamma - 1)^2\lambda q}{\gamma \sin\beta(\gamma + 2\cos^2\beta - 1)^2}\right] \quad (4d)$$

The leading order terms in Eqs. (4a–d), which will be denoted by the subscript s, represent the inert oblique shock solution in the hypersonic limit. Thus, for example, the leading order pressure and density are P_s and ρ_s, respectively. The angle θ given in Eq. (4d) represents the local flow angle and for $\lambda = 1$, the wedge angle. The $\mathcal{O}(\varepsilon)$ correction terms account for corrections away from the hypersonic limit and for chemical reaction effects. For $\gamma > 1$, exothermic reaction, $q > 0$, and $0 < \beta < \pi/2$, the bracketed terms in Eqs. (4a–d) are strictly positive. Thus, exothermic reaction and finite Mach number effects tend to decrease the pressure, decrease the density, increase the velocity magnitude, and broaden the angle between the discontinuity and solid surface.

A maximum wedge angle θ, dependent only on γ in the hypersonic limit, is implied by Eq. (4d). At leading order, this equation can be written as a quadratic equation in $\sin\beta$. The discriminant of this quadratic provides a condition for real solutions, which restricts the wedge angle to be below a maximum value. Wedge angles greater than the maximum give rise to a detached bow shock. In the hypersonic limit, the corresponding conditions on the wedge and shock angles

θ and β for an attached shock are

$$\theta \leq \sin^{-1}\left(\frac{1}{\gamma}\right) \tag{5a}$$

$$\beta \leq \sin^{-1}\left(\sqrt{\frac{\gamma+1}{2\gamma}}\right) \tag{5b}$$

For $\gamma = 1.4$, this corresponds to $\theta \leq 45.6$ deg and $\beta \leq 67.8$ deg. The CJ wedge angle, which provides a lower bound on θ for a structure with a lead shock followed by a one-step reaction, is $\mathcal{O}(\varepsilon)$ in the hypersonic limit; Pratt et al.[1] give a complete determination away from the hypersonic limit.

Perturbation Equations

The inert oblique shock solution suggests a more convenient coordinate system $[(x,y) \rightarrow (\xi,\eta), (u,v) \rightarrow (U,V)]$ in which the unit position and velocity vectors are parallel to the leading order shock and wall. It will be seen that, as a result of this choice, first integrals of the leading order product mass fraction equation and $\mathcal{O}(\varepsilon)$ streamwise momentum equation can be obtained. In addition, the shock and wall boundary conditions are transferred to $\xi = 0$, $\eta = 0$, respectively. The appropriate linear transformations and inverse transformations are

$$x = \xi\cos\theta + \eta\cos\beta_s, \quad y = \xi\sin\theta + \eta\sin\beta_s$$

$$u = U\cos\theta + V\cos\beta_s, \quad v = U\sin\theta + V\sin\beta_s$$

$$\xi = \frac{x\sin\beta_s - y\cos\beta_s}{\sin\alpha}, \quad \eta = \frac{y\cos\theta - x\sin\theta}{\sin\alpha}$$

$$U = \frac{u\sin\beta_s - v\cos\beta_s}{\sin\alpha}, \quad V = \frac{v\cos\theta - u\sin\theta}{\sin\alpha} \tag{6}$$

where ξ and U are the distance and velocity, respectively, measured parallel to the wall, and η and V are the distance and velocity, respectively, measured parallel to the straight shock found in the hypersonic limit (see Fig. 1). Here, β_s is the leading order shock angle, and α is defined as the angle between the leading order inert shock and wedge; $\alpha = \beta_s - \theta$. The direction parallel to the wall is called the streamwise direction and the direction parallel to the shock the transverse direction.

With these transformations, Eqs. (2a–i) can be written as follows:

$$\frac{\partial}{\partial\xi}(\rho U) + \frac{\partial}{\partial\eta}(\rho V) = 0 \tag{7a}$$

$$\rho U\left(\frac{\partial U}{\partial\xi} + \cos\alpha\frac{\partial V}{\partial\xi}\right) + \rho V\left(\frac{\partial U}{\partial\eta} + \cos\alpha\frac{\partial V}{\partial\eta}\right) + \frac{\partial P}{\partial\xi} = 0 \tag{7b}$$

$$\rho U\left(\cos\alpha\frac{\partial U}{\partial\xi} + \frac{\partial V}{\partial\xi}\right) + \rho V\left(\cos\alpha\frac{\partial U}{\partial\eta} + \frac{\partial V}{\partial\eta}\right) + \frac{\partial P}{\partial\eta} = 0 \tag{7c}$$

$$U\frac{\partial P}{\partial\xi} + V\frac{\partial P}{\partial\eta} - \gamma\frac{P}{\rho}\left(U\frac{\partial\rho}{\partial\xi} + V\frac{\partial\rho}{\partial\eta}\right) = \varepsilon(\gamma-1)q\rho(1-\lambda)e^{-\varepsilon\Theta\rho/P} \tag{7d}$$

$$U\frac{\partial\lambda}{\partial\xi} + V\frac{\partial\lambda}{\partial\eta} = (1-\lambda)e^{-\varepsilon\Theta\rho/P} \tag{7e}$$

$$\xi_s = \frac{-1}{\sin\alpha}\int_0^\eta \sin[\beta(s) - \beta_s]\,ds \tag{7f}$$

$$\frac{V}{U} = \frac{d\Omega(\xi)}{d\xi} \quad \text{on} \quad \eta = \Omega(\xi) \tag{7g}$$

$$\omega_z = \csc\alpha\left[\left(\frac{\partial V}{\partial\xi} - \frac{\partial U}{\partial\eta}\right) + \cos\alpha\left(\frac{\partial U}{\partial\xi} - \frac{\partial V}{\partial\eta}\right)\right] \tag{7h}$$

$$\kappa = \frac{d\beta(\eta)}{d\eta} \tag{7i}$$

Here, $\Omega(\xi)$ is a function found by transforming the function $W(x)$ to $\xi - \eta$ space. It is assumed that all variables can be written in a regular expansion, uniformly valid in a region bounded within $\mathcal{O}(1)$ distances from the wedge tip, in which ε is taken to be a small parameter:

$$P = P_s + \varepsilon P' + \mathcal{O}(\varepsilon^2), \quad \rho = \rho_s + \varepsilon\rho' + \mathcal{O}(\varepsilon^2)$$

$$U = U_s + \varepsilon U' + \mathcal{O}(\varepsilon^2), \quad \kappa = \varepsilon\kappa' + \mathcal{O}(\varepsilon^2)$$

$$V = \varepsilon V' + \mathcal{O}(\varepsilon^2), \quad \beta = \beta_s + \varepsilon\beta' + \mathcal{O}(\varepsilon^2)$$

$$\lambda = \lambda_s + \mathcal{O}(\varepsilon), \quad \Omega = \varepsilon\Omega' + \mathcal{O}(\varepsilon^2)$$

$$\omega_z = \varepsilon\omega_z' + \mathcal{O}(\varepsilon^2) \tag{8}$$

The asymptotic shock conditions and definitions of supplementary constants U_s, A, B, C, D, E, and F are given next. The $\mathcal{O}(\varepsilon)$ correction accounts for finite Mach number and shock curvature:

$$U(0,\eta) = U_s + \varepsilon(B + C\beta'(\eta)) + \mathcal{O}(\varepsilon^2)$$

$$V(0,\eta) = \varepsilon(A + D\beta'(\eta)) + \mathcal{O}(\varepsilon^2)$$

$$P(0,\eta) = P_s + \varepsilon(E + F\beta'(\eta)) + \mathcal{O}(\varepsilon^2)$$

$$U_s = \sqrt{u_s^2 + v_s^2} = \frac{\sqrt{\gamma}\sqrt{\gamma^2 + 2\gamma\cos2\beta_s + 1}}{\gamma+1}$$

$$A = -\frac{2\sqrt{\gamma}\cos\beta_s}{(\gamma-1)\sin^2\beta_s}$$

$$B = \frac{2\sqrt{\gamma}\sqrt{\gamma^2 + 2\gamma\cos2\beta_s + 1}}{(\gamma^2-1)\sin^2\beta_s}$$

$$C = -\frac{2\sqrt{\gamma}\sqrt{\gamma^2 + 2\gamma\cos2\beta_s + 1}}{(\gamma^2-1)\tan\beta_s}$$

$$D = \frac{2\sqrt{\gamma}(\gamma\cos2\beta_s + 1)}{(\gamma^2-1)\sin\beta_s}, \quad E = -\frac{\gamma-1}{\gamma+1}$$

$$F = \frac{2\gamma\sin2\beta_s}{(\gamma+1)} \tag{9}$$

At leading order, the forcing term in the energy equation (7d) is zero, and Eqs. (7a–d,f–i) are satisfied by the constant inert oblique state: $P \approx P_s$, $U \approx U$, $V \approx 0$, $\rho \approx \rho_s$, $\beta \approx \beta_s$, $\Omega \approx 0$, $\omega_z \approx 0$, $\kappa \approx 0$. Equation (7e), however, has a nontrivial solution at leading order, $\lambda_s \approx 1 - \exp(-\xi/U_s)$. After the shock, the reaction commences, and heat is released at the rate dictated by the local postshock conditions. In the leading order approximation, the heat release does not affect the flow properties. As a result, the reaction rate, which in general is a function of density, pressure, and extent of reaction, varies only as the extent of reaction in the reaction zone. The dimensional leading order reaction zone length is only a function of the postshock velocity and the Arrhenius prefactor. As the postshock velocity is of the same order as the undis-

turbed velocity, and γ and β_s are $\mathbb{O}(1)$, the dimensional reaction zone length is estimated as $L = \mathbb{O}(u_o/r_o)$. For different ordering schemes [for instance, $\Theta = \mathbb{O}(1/\varepsilon)$] the reaction zone length would be a function of the activation energy also, but would change at most by a constant factor as the exponential Arrhenius term is constant at $\mathbb{O}(1)$ in the hypersonic limit.

At $\mathbb{O}(\varepsilon)$ heat release influences flowfield. Equations (7b–d) can be written compactly by using the solution for λ_s to substitute for λ in Eq. (7d) and using Eq. (7a) to replace density derivatives by velocity derivatives in Eq. (7d):

$$\rho_s U_s\left(\frac{\partial U'}{\partial \xi} + \cos\alpha \frac{\partial V'}{\partial \xi}\right) + \frac{\partial P'}{\partial \xi} = 0 \tag{10a}$$

$$\rho_s U_s\left(\cos\alpha \frac{\partial U'}{\partial \xi} + \frac{\partial V'}{\partial \xi}\right) + \frac{\partial P'}{\partial \eta} = 0 \tag{10b}$$

$$U_s \frac{\partial P'}{\partial \xi} + \gamma P_s\left(\frac{\partial U'}{\partial \xi} + \frac{\partial V'}{\partial \eta}\right) = (\gamma - 1)\rho_s q e^{-\xi/U_s} \tag{10c}$$

At this order, the initial conditions, to be applied just past the shock, are $U' = B + C\beta'(\eta)$, $V' = A + D\beta'(\eta)$, and $P' = E + F\beta'(\eta)$. The shock angle $\beta'(\eta)$ is chosen so the downstream boundary condition is satisfied. At $\mathbb{O}(\varepsilon)$, the shock location ξ_s and downstream boundary condition are given by

$$\xi_s = -\frac{\varepsilon}{\sin\alpha}\int_0^\eta \beta'(s)\, ds \tag{10d}$$

$$V' = U_s \frac{d\Omega'}{d\xi} \qquad \text{on} \qquad \eta = \Omega'(\xi) \tag{10e}$$

The equations are uncoupled from the $\mathbb{O}(\varepsilon)$ density; consequently, the mass equation, which fixes the density, is unnecessary when the pressure and velocity fields are calculated. The linear constant coefficient equations and initial and boundary conditions can thus be written as a complete set of five coupled equations [Eqs. (10a–e)] in the five unknowns P', U', V', β', and either $\xi_s(\eta)$ or $\Omega(\xi)$.

Straight-Shock Curved-Wall Solution

By specifying the shock position ξ_s as a straight line attached to a curved wall of unknown shape $\Omega(\xi)$, a solution to Eqs. (10a–e) can be obtained. Two simplifying features of the solution distinguish it from the more complicated case of a curved shock attached to a straight wall. The flowfield is irrotational and only a function of the streamwise coordinate ξ, whereas the curved-shock straight-wall solution is both rotational and a function of both spatial variables ξ and η. The solution obtained in this section can also describe the flowfield in the curved-shock straight-wall problem in the limit as $\eta \to \infty$, described in a later section. In this limit, the curvature of the shock approaches zero; thus, the analysis of this section is appropriate.

With the assumption of no $\mathbb{O}(\varepsilon)$ shock deflection, $\beta'(\eta) \equiv 0$. The shock location and shock conditions simplify to $\xi_s = 0$, $U' = B$, $V' = A$, and $P' = E$. With the constant postshock Mach number defined as $M_s^2 = \rho_s U_s^2/(\gamma P_s) = (\gamma^2 + 2\gamma\cos 2\beta_s + 1)/[2\gamma(\gamma - 1)\sin^2\beta_s]$, the following velocity and pressure fields satisfy Eqs. (10a–c):

$$U' = \frac{M_s^2(\gamma - 1)q}{U_s(1 - M_s^2\sin^2\alpha)}[1 - e^{-\xi/U_s}] + B$$

$$= \frac{\sqrt{\gamma^2 + 2\gamma\cos 2\beta_s + 1}}{\sqrt{\gamma}\sin^2\beta_s} \times \left[(1 - e^{-\xi/U_s})q + \frac{2\gamma}{\gamma^2 - 1}\right] \tag{11a}$$

$$V' = -\frac{M_s^2(\gamma - 1)\cos\alpha\, q}{U_s(1 - M_s^2\sin^2\alpha)}[1 - e^{-\xi/U_s}] + A$$

$$= -\frac{(\gamma + 1)\cos\beta_s}{\sqrt{\gamma}\sin^2\beta_s}\left[(1 - e^{-\xi/U_s})q + \frac{2\gamma}{\gamma^2 - 1}\right] \tag{11b}$$

$$P' = -\frac{\rho_s M_s^2(\gamma - 1)\sin^2\alpha\, q}{1 - M_s^2\sin^2\alpha}[1 - e^{-\xi/U_s}] + E$$

$$= -(\gamma - 1)\left[(1 - e^{-\xi/U_s})q + \frac{1}{\gamma + 1}\right] \tag{11c}$$

The solution (11a–c) is written in two forms. The first form, given in terms of the shocked state, can easily be shown to satisfy Eqs. (10a–c) and initial conditions by direct substitution. The second form is found by using the definitions in Eqs. (9) to evaluate the constants that appear in the first form in terms of more basic parameters. With the second form, it is seen that as $\xi \to \infty$ that the pressure perturbations exactly match those predicted at $\mathbb{O}(\varepsilon)$ by the Rankine-Hugoniot analysis [Eq. (4a)]. It can further be shown, by using Eqs. (11a) and (11b) to determine the velocity perturbation magnitude and the mass equation (7a) to determine the density perturbation, that as $\xi \to \infty$ these variables exactly match values predicted by the Rankine-Hugoniot analysis [Eqs. (4b) and (4c)] at $\mathbb{O}(\varepsilon)$.

Other aspects of the description of an oblique detonation deduced from consideration of the Rankine-Hugoniot analysis are confirmed. The velocity tangent to the shock wave, $V_t = U_s\cos\alpha + \varepsilon[U'\cos\alpha + V']$, is a constant, whereas the velocity normal to the shock wave, $V_n = U_s\sin\alpha + \varepsilon[U'\sin\alpha]$, varies with distance. Using the mass equation to determine density variation, and using this in conjunction with the velocity component normal to the shock wave, allows the Mach number normal to the shock wave M_n to be determined. It is seen for $\gamma > 1$ that M_n is initially subsonic, increases as chemical reaction occurs, but for $\mathbb{O}(1)$ heat release q remains subsonic. The structures of V_t, V_n, and M_n^2 are as follows:

$$V_t = \sqrt{\gamma}\cos\beta_s + \mathbb{O}(\varepsilon^2) \tag{11d}$$

$$V_n = \frac{\sqrt{\gamma}(\gamma - 1)\sin\beta_s}{\gamma + 1} + \varepsilon\frac{\gamma - 1}{\sqrt{\gamma}\sin\beta_s}\left[(1 - e^{-\xi/U_s})q + \frac{2\gamma}{\gamma^2 - 1}\right] + \mathbb{O}(\varepsilon^2) \tag{11e}$$

$$M_n^2 = \frac{\gamma - 1}{2\gamma} + \varepsilon\frac{(\gamma + 1)^2(\gamma - 1)}{4\gamma^2\sin^2\beta_s} \times \left[(1 - e^{-\xi/U_s})q + \frac{1}{\gamma - 1}\right] + \mathbb{O}(\varepsilon^2) \tag{11f}$$

In light of Eqs. (11d–f), the idea that an oblique detonation can be described by superimposing a constant velocity field onto a one-dimensional detonation structure is confirmed. This could be more directly exhibited by choosing an orthogonal coordinate system oriented to the shock; the method used here is chosen so that this simple case can be examined in the same way as the straight-wall curved-shock case, for which the present formulation is advantageous.

A wall shape consistent with this flowfield can be found by determining the streamline that passes through the origin. Streamlines are defined by the differential equation, given here in both the Cartesian and transformed coordinate system, valid at all orders, $dx/u = dy/v$, $d\xi/U = d\eta/V$. The now determined velocities are substituted into this equation, and the condition $\eta(0) = 0$ is taken so that the wall streamline passes through the origin. These substitutions and subsequent

integration yield an expression for the wall shape perturbation:

$$\Omega'(\xi) = \frac{(\gamma + 1)\cos\beta_s}{\sqrt{\gamma}\sin^2\beta_s} q\left(1 - e^{-\xi/U_s} - \frac{\xi}{U_s}\right) - \frac{2(\gamma + 1)\cos\beta_s\xi}{(\gamma - 1)\sin^2\beta_s\sqrt{\gamma^2 + 2\gamma\cos 2\beta_s + 1}} \quad (11g)$$

From Eq. (11g), it is seen that a far-field nonuniformity exists. When $\xi = \mathcal{O}(1/\varepsilon)$, the leading order terms are of the same order as terms at the following order. That is, for distances far from the wedge tip [$\xi = \mathcal{O}(1/\varepsilon)$], the wall is deflected by an $\mathcal{O}(1)$ distance. The solution is thus only uniformly valid in a spatial domain bounded by $\mathcal{O}(1)$ distances from the wedge tip. Finally, it is seen from the definitions of vorticity and shock curvature that both are zero for this flowfield.

Results are given for a) a strong oblique detonation inclined at $\beta = \pi/2.12$ and b) an overdriven weak oblique detonation inclined at $\beta = \pi/3$. In both cases, $q = 11.2$ and $\varepsilon = 0.0237$ ($M_o = 6.5$). Both paths of the reaction are sketched in Fig. 2, proceeding from N to S. All results can be returned to Cartesian space by use of Eqs. (6). Streamlines are plotted in Figs. 3a and 3b. The streamline that passes through the origin gives the shape of the wall. Other streamlines are formed by translating the wall streamline such that the streamlines begin at the shock. The dimensionless pressure, streamwise and transverse velocities, Mach number normal to the shock, and product mass fraction are plotted vs streamwise distance in Figs. 4a and 4b. The more powerful shock of the strong oblique detonation gives rise to short relaxation zones relative to the overdriven weak oblique detonation.

Though the issue of what boundary conditions are necessary for a well-posed, stable solution has not been addressed, analogs with inert flow offer plausible suggestions. For external flow over a finite wedge, the far-field disturbance must be a Mach wave, which suggests that the near-field solution should be the overdriven weak solution so that the proper matching can occur. The strong oblique detonation may be appropriate for an internal duct flow with a sufficiently high backpressure and walls that are parallel to the streamlines. The analog here is a normal shock standing in a one-dimensional duct.

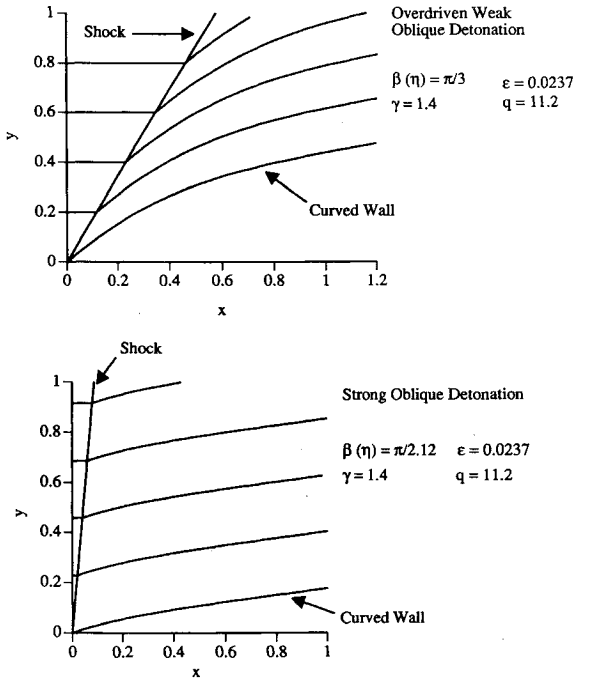

Fig. 3 Shock locus and streamlines for irrotational straight-shock curved-wall case: a) overdriven weak; b) strong.

Straight-Wall Curved-Shock Solution

The more difficult problem posed by Eqs. (10a–e), namely, finding the shock shape and reactive flowfield associated with a straight wall, is now considered. In this problem, the downstream boundary condition is given by the known wall shape and is specified so that on the wall there is no transverse velocity component, i.e., $V' = 0$ on $\eta = 0$. To accommodate the shock boundary condition, a change of variables so that the shock is located at $\zeta = 0$ is advantageous:

$$\zeta = \xi + \frac{\varepsilon}{\sin\alpha}\int_0^\eta \beta(s)\,ds \quad (12)$$

With this transformation, the linear partial differential equations (10a–c) remain unchanged in form at $\mathcal{O}(\varepsilon)$; that is, they may be written in terms of ζ by simply replacing ξ by ζ at every occurrence. The shock conditions are to be applied at $\zeta = 0$.

The transformed momentum equation (10a) can be integrated with respect to ζ. An arbitrary function of η arises as a result that is fixed in terms of the arbitrary shock-shape function $\beta'(\eta)$ when the shock conditions are applied. The integrated equation is written as follows so that pressure is given as a function of the velocities and shock shape (the constants G and H are defined below the pressure equation):

$$P' = -\rho_s U_s(U' + \cos\alpha V') + G + \rho_s U_s H\beta'(\eta) \quad (13)$$

$$G = \rho_s U_s(B + \cos\alpha A) + E = 1$$

$$H = C + D\cos\alpha + \frac{F}{\rho_s U_s} = -\frac{2\sqrt{\gamma}\sin 2\beta_s}{(\gamma + 1)\sqrt{\gamma^2 + 2\gamma\cos 2\beta_s + 1}}$$

Equation (13) can be used to determine the partial derivatives of pressure in terms of velocity derivatives and the shock curvature. These results are then substituted into Eqs. (10a)

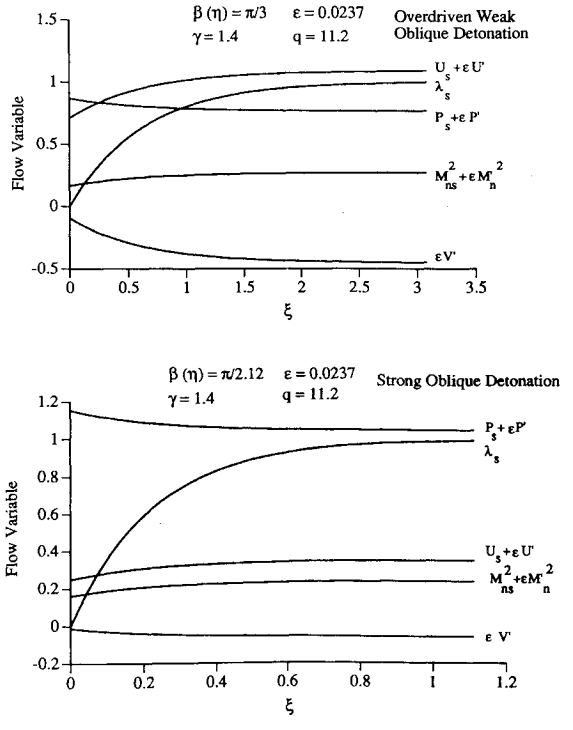

Fig. 4 Flow variables vs streamwise distance for irrotational straight-shock curved-wall case: a) overdriven weak; b) strong.

and (10b) to give

$$\left(\frac{\partial V'}{\partial \zeta} - \frac{\partial U'}{\partial \eta}\right) + \cos\alpha\left(\frac{\partial U'}{\partial \zeta} - \frac{\partial V'}{\partial \eta}\right) = -H\frac{d\beta'(\eta)}{d\eta} \quad (14a)$$

$$-\frac{\partial U'}{\partial \zeta} - \cos\alpha\frac{\partial V'}{\partial \zeta} + \frac{1}{M_s^2}\left(\frac{\partial U'}{\partial \zeta} + \frac{\partial V'}{\partial \eta}\right) = \frac{(\gamma - 1)q}{U_s^2}\exp(-\zeta/U_s) \quad (14b)$$

Equation (14a) can be rewritten in terms of vorticity and shock curvature as $\omega_z' = -H\kappa'(\eta)/\sin\alpha = 4\gamma^{1/2}\cos\beta_s\kappa'(\eta)/(\gamma^2 - 1)$; consequently, $\partial\omega_z'/\partial\zeta = 0$. Thus, for $\gamma > 1$, $0 < \beta_s < \pi/2$, and $\kappa' = d\beta'/d\eta > 0$, corresponding to a shock that bends away from the wedge, a strictly positive vorticity, generated at the shock front and proportional to the shock curvature, is convected along streamlines and remains constant on the streamlines. The local shock curvature will be seen to be dependent on the heat release, material properties, and undisturbed conditions.

Equations (14a) and (14b) are rewritten in characteristic form, using the associated definitions of the characteristics λ_+, λ_- and constants a_1, a_2, b_1, b_2, and c_1:

$$a_1\left[\frac{\partial U'}{\partial \zeta} + \lambda_+\frac{\partial U'}{\partial \eta}\right] + b_1\left[\frac{\partial V'}{\partial \zeta} + \lambda_+\frac{\partial V'}{\partial \eta}\right] = -H\kappa'(\eta) + c_1 e^{-\zeta/U_s} \quad (15a)$$

$$a_2\left[\frac{\partial U'}{\partial \zeta} + \lambda_-\frac{\partial U'}{\partial \eta}\right] + b_2\left[\frac{\partial V'}{\partial \zeta} + \lambda_-\frac{\partial V'}{\partial \eta}\right] = -H\kappa'(\eta) - c_1 e^{-\zeta/U_s} \quad (15b)$$

$$\lambda_+ = \frac{\cos\alpha + \sin\alpha\sqrt{M_s^2 - 1}}{M_s^2\sin^2\alpha - 1}, \quad \lambda_- = \frac{\cos\alpha - \sin\alpha\sqrt{M_s^2 - 1}}{M_s^2\sin^2\alpha - 1}$$

$$a_1 = \cos\alpha - \sin\alpha\sqrt{M_s^2 - 1}, \quad a_2 = \cos\alpha + \sin\alpha\sqrt{M_s^2 - 1}$$

$$b_1 = 1 - \frac{M_s^2\sin\alpha\cos\alpha}{\sqrt{M_s^2 - 1}}, \quad b_2 = 1 + \frac{M_s^2\sin\alpha\cos\alpha}{\sqrt{M_s^2 - 1}}$$

$$c_1 = \frac{M_s^2(\gamma - 1)\sin\alpha}{U_s^2\sqrt{M_s^2 - 1}}q$$

The characteristics are real for sonic or supersonic postshock Mach number, $M_s^2 \geq 1$, and under this condition can be shown to be strictly negative. It can also be shown by setting $M_s^2 = (\gamma^2 + 2\gamma\cos 2\beta_s + 1)/[2\gamma(\gamma - 1)\sin^2\beta_s] \geq 1$ that the condition for an attached shock [Eq. (5b)] is necessary and sufficient for real characteristics. The characteristic form suggests another variable change that facilitates integration of Eqs. (15a) and (15b); let l and m be defined such that $l = \eta - \lambda_+\zeta$, $m = \eta - \lambda_-\zeta$. Under this change of variables, Eqs. (15a) and (15b) are written as follows:

$$a_1\frac{\partial U'}{\partial m} + b_1\frac{\partial V'}{\partial m} = -\frac{H}{\lambda_+ - \lambda_-}\kappa'\left(\frac{\lambda_+ m - \lambda_- l}{\lambda_+ - \lambda_-}\right) + \frac{c_1}{\lambda_+ - \lambda_-}\exp\left[\frac{-(m - l)}{\lambda_+ - \lambda_-}\frac{1}{U_s}\right] \quad (16a)$$

$$a_2\frac{\partial U'}{\partial l} + b_2\frac{\partial V'}{\partial l} = \frac{H}{\lambda_+ - \lambda_-}\kappa'\left(\frac{\lambda_+ m - \lambda_- l}{\lambda_+ - \lambda_-}\right) + \frac{c_1}{\lambda_+ - \lambda_-}\exp\left[\frac{-(m - l)}{\lambda_+ - \lambda_-}\frac{1}{U_s}\right] \quad (16b)$$

Equations (16a) and (16b) can be integrated with respect to m and l, respectively, to form the following equations in which $f(l)$ and $g(m)$ appear as arbitrary functions:

$$a_1U' + b_1V' = -\frac{H}{\lambda_+}\beta'\left(\frac{\lambda_+ m - \lambda_- l}{\lambda_+ - \lambda_-}\right) - c_1U_s\exp\left[\frac{-(m - l)}{\lambda_+ - \lambda_-}\frac{1}{U_s}\right] + f(l) \quad (17a)$$

$$a_2U' + b_2V' = -\frac{H}{\lambda_-}\beta'\left(\frac{\lambda_+ m - \lambda_- l}{\lambda_+ - \lambda_-}\right) + c_1U_s\exp\left[\frac{-(m - l)}{\lambda_+ - \lambda_-}\frac{1}{U_s}\right] + g(m) \quad (17b)$$

Next, the shock conditions are used to express the functions f and g in terms of the shock shape function β'. At the shock front, $\zeta = 0$ and, correspondingly, $l = m$. The parameter t is defined so that $t = l = m = \eta$ at $\zeta = 0$. By applying the shock conditions, it is found that

$$f(t) = a_1[B + C\beta'(t)] + b_1[A + D\beta'(t)] + \frac{H}{\lambda_+}\beta'(t) + c_1U_s \quad (18a)$$

$$g(t) = a_2[B + C\beta'(t)] + b_2[A + D\beta'(t)] + \frac{H}{\lambda_-}\beta'(t) - c_1U_s \quad (18b)$$

The shock angle perturbation β' is determined by applying the wall boundary condition. For $\eta = 0$, s is defined such that $l = s$, $m = (\lambda_-/\lambda_+)s$. Setting $V' = 0$ on $\eta = 0$ in Eqs. (17a) and (17b) yields

$$a_1U' = -\frac{H}{\lambda_+}\beta'(0) - c_1U_s\exp\left(\frac{s}{\lambda_+U_s}\right) + f(s) \quad (19a)$$

$$a_2U' = -\frac{H}{\lambda_-}\beta'(0) + c_1U_s\exp\left(\frac{s}{\lambda_+U_s}\right) + g\left(\frac{\lambda_-}{\lambda_+}s\right) \quad (19b)$$

If the streamwise velocity is eliminated from Eqs. (19a) and (19b) and Eqs. (18a) and (18b) are used to write the functions f and g in terms of β', a single equation can be written with the function β' as the only unknown. This equation along with definitions of constants A_1, A_2, A_3, A_4, and A_5 is

$$A_1\beta'\left(\frac{\lambda_-}{\lambda_+}s\right) + A_2\beta'(s) + A_3\exp\left(\frac{s}{\lambda_+U_s}\right) + A_4\beta'(0) + A_5 = 0 \quad (20)$$

$$A_1 = \frac{a_1H}{\lambda_-} + a_1a_2C + a_1b_2D$$

$$A_2 = -\left(\frac{a_2H}{\lambda_+} + a_1a_2C + a_2b_1D\right)$$

$$A_3 = U_sc_1(a_1 + a_2), \quad A_4 = H(a_2/\lambda_+ - a_1/\lambda_-) = 0$$

$$A_5 = A(a_1b_2 - a_2b_1) - U_sc_1(a_1 + a_2)$$

Equations of this class are also found by Spence,[6] Lee,[12] and Fickett.[26] To evaluate this function, each term in Eq. (20) is

expanded in a Taylor series about $s = 0$:

$$(A_1 + A_2)\beta'(0) + \sum_{n=1}^{\infty}\left\{\frac{s^n}{n!}\left[A_1\left(\frac{\lambda_-}{\lambda_+}\right)^n\frac{d^n\beta'(s)}{ds^n} + A_2\frac{d^n\beta'(s)}{ds^n} + \frac{A_3}{(\lambda_+U_s)^n}\right]\right\} + A_3 + A_5 = 0 \tag{21}$$

To satisfy Eq. (21) for all s, it is required that

$$\beta'(0) = -\frac{A_3 + A_5}{A_1 + A_2} \tag{22a}$$

$$\frac{d^n\beta'(s)}{ds^n} = -\frac{A_3}{U_s^n(A_1\lambda_-^n + A_2\lambda_+^n)} \tag{22b}$$

Equations (22) contain sufficient information to express the shock angle perturbations as a Taylor series expanded about $s = 0$. Evaluating this series at $s = \eta$ and adding the result to the leading order solution allows the total shock deflection angle to be written as

$$\begin{aligned}\beta(\eta) &= \beta_s - \varepsilon\left[\frac{A_3 + A_5}{A_1 + A_2} + A_3\sum_{n=1}^{\infty}\frac{1}{n!}\left(\frac{\eta}{U_s}\right)^n\frac{1}{A_1\lambda_-^n + A_2\lambda_+^n}\right] + \mathcal{O}(\varepsilon^2)\\ &= \beta_s - \varepsilon\left\{\frac{A_5}{A_1 + A_2} + \frac{A_3}{A_2}\sum_{n=0}^{\infty}(-1)^n\left(\frac{A_1}{A_2}\right)^n \times \exp\left[\frac{\eta}{U_s\lambda_+}\left(\frac{\lambda_-}{\lambda_+}\right)^n\right]\right\} + \mathcal{O}(\varepsilon^2)\end{aligned} \tag{23}$$

The second form, given in terms of an expansion of exponentials, is obtained from the first form by expanding the term $1/(A_1\lambda_-^n + A_2\lambda_+^n)$ in an infinite series and evaluating each term in terms of an exponential. For convergence, it is required that $|A_1/A_2| < 1$. Because of the complicated algebraic forms, it is difficult to find explicit conditions for $|A_1/A_2| < 1$; however, numerical evaluation for specific cases showed that the condition was always satisfied. For $\eta \geq 0$, the arguments of the exponentials in Eqs. (23) are negative; consequently, the exponentials are ≤ 1. The series can thus be bounded, and application of the Weierstrass M test shows that the series converges absolutely and uniformly.

By examining the first form of the series, it can be shown that the shock angle perturbation can be expressed as the sum of a constant and the product of heat release q and a function of η, β_s, and γ. This is because the term $(A_3 + A_5)/(A_1 + A_2)$ is independent of q, whereas the term A_3 is proportional to q. From the second form, it is seen that the shock angle pertubations converge to a limiting value as η approaches infinity. This limiting value of the shock perturbation is given in terms of A_1, A_2, and A_5, and also in terms of more fundamental parameters:

$$\begin{aligned}\beta'(\infty) &= -\frac{A_5}{A_1 + A_2}\\ &= \frac{(\gamma + 1)\cos\beta_s}{\sin\beta_s(\gamma\cos 2\beta_s + 1)}\left[1 + \frac{\gamma^2 - 1}{2\gamma}q\right]\end{aligned} \tag{24}$$

It is not expected that this expression matches an equivalent expression predicted from Rankine-Hugoniot analysis. This is because the Rankine-Hugoniot analysis assumes a constant velocity tangent to the original shock, whereas the tangential velocity changes throughout the reaction zone in the straight-wall curved-shock problem.

Integration and differentiation, respectively, of Eqs. (23) give ξ_s and κ explicitly:

$$\xi_s(\eta) = \varepsilon\frac{U_s}{\sin\alpha}\left[\frac{A_5}{A_1 + A_2}\left(\frac{\eta}{U_s}\right) + \frac{A_3\lambda_+}{A_2}\left\{\frac{-1}{1 + (A_1/A_2)(\lambda_+/\lambda_-)} + \sum_{n=0}^{\infty}(-1)^n\left(\frac{A_1}{A_2}\right)^n\left(\frac{\lambda_+}{\lambda_-}\right)^n \exp\left[\frac{\eta}{U_s\lambda_+}\left(\frac{\lambda_-}{\lambda_+}\right)^n\right]\right\}\right] + \mathcal{O}(\varepsilon^2) \tag{25a}$$

$$\kappa(\eta) = -\varepsilon\frac{A_3}{A_2U_s\lambda_+}\sum_{n=0}^{\infty}(-1)^n\left(\frac{A_1}{A_2}\right)^n\left(\frac{\lambda_-}{\lambda_+}\right)^n \exp\left[\frac{\eta}{U_s\lambda_+}\left(\frac{\lambda_-}{\lambda_+}\right)^n\right] + \mathcal{O}(\varepsilon^2) \tag{25b}$$

These series were also convergent for all cases studied. The shock curvature can be shown to be a product of the heat release q and a function of η, β_s, and γ. The curvature has a maximum value at $\eta = 0$ and approaches zero as η approaches infinity. The vorticity, equal to the curvature at this order, is maximum along the wall and confined to a layer of $\mathcal{O}(1)$ thickness next to the wall. This vorticity layer is equivalent to an entropy layer (cf. Lee[12] or Capiaux and Washington[8]). Perturbations of shock curvature and deviation of the shock angle perturbation from its initial perturbation, both scaled by heat release, are plotted vs the distance along the shock wave η in Fig. 5 for $\gamma = 1.4$, $\beta_s = \pi/3$.

With knowledge of the function β', it is possible to construct all other flowfield variables. To construct the velocity field, Eq. (18a) is used to evaluate $f(t)$ at $t = l$ and Eq. (18b) is used to evaluate $g(t)$ at $t = m$. The results are substituted into Eqs. (17a) and (17b) so that U' and V' are written as functions of l and m. Then, l and m can be eliminated in favor of ζ and η so that Eqs. (17a) and (17b) may be written in the form given next [definitions of the functions $R_1(\zeta,\eta)$ and $R_2(\zeta,\eta)$ follow]:

$$a_1U' + b_1V' = R_1(\zeta,\eta) \tag{26a}$$

$$a_2U' + b_2V' = R_2(\zeta,\eta) \tag{26b}$$

$$\begin{aligned}R_1(\zeta,\eta) &= -\frac{H}{\lambda_+}\beta'(\eta) - c_1U_s\exp(-\zeta/U_s)\\ &\quad + (a_1B + b_1A + c_1U_s)\\ &\quad + \beta'(\eta - \lambda_+\zeta)\left(a_1C + b_1D + \frac{H}{\lambda_+}\right)\end{aligned}$$

$$\begin{aligned}R_2(\zeta,\eta) &= -\frac{H}{\lambda_-}\beta'(\eta) + c_1U_s\exp(-\zeta/U_s)\\ &\quad + (a_2B + b_2A - c_1U_s)\\ &\quad + \beta'(\eta - \lambda_-\zeta)\left(a_2C + b_2D + \frac{H}{\lambda_-}\right)\end{aligned}$$

Equations (26a) and (26b) may be uncoupled to form explicit expressions for the velocities:

$$U' = \frac{b_2R_1(\zeta,\eta) - b_1R_2(\zeta,\eta)}{a_1b_2 - a_2b_1} \tag{27a}$$

$$V' = \frac{a_1 R_2(\zeta,\eta) - a_2 R_1(\zeta,\eta)}{a_1 b_2 - a_2 b_1} \tag{27b}$$

With the known U', V', and β', Eq. (13) can be used to determine the pressure field.

The shock shape and streamlines for a representative straight-wall curved-shock problem are plotted in Fig. 6. Parameters for this case, chosen so the shock curvature can be visually identified, are $q = 11.2$, $\theta = \pi/4.197$, $\gamma = 1.4$, and $\varepsilon = 0.01$. Although in principle it is possible to determine an analytic expression for the streamlines since the velocity field is known, the algebra is lengthy. As such, the streamlines are determined by converting the velocity field, $U(\zeta,\eta)$, $V(\zeta,\eta)$ given by Eqs. (27a) and (27b) to Cartesian space $u(x,y)$, $v(x,y)$ and

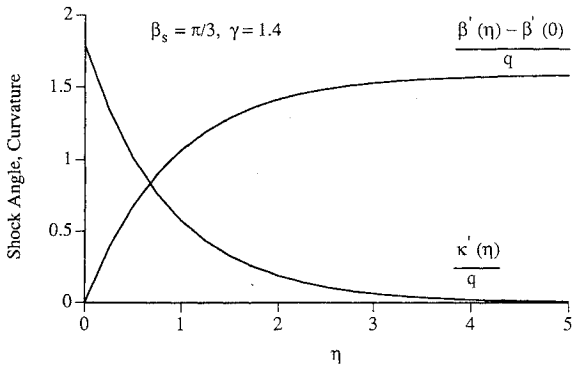

Fig. 5 Shock angle and curvature perturbations scaled by heat release vs distance along shock.

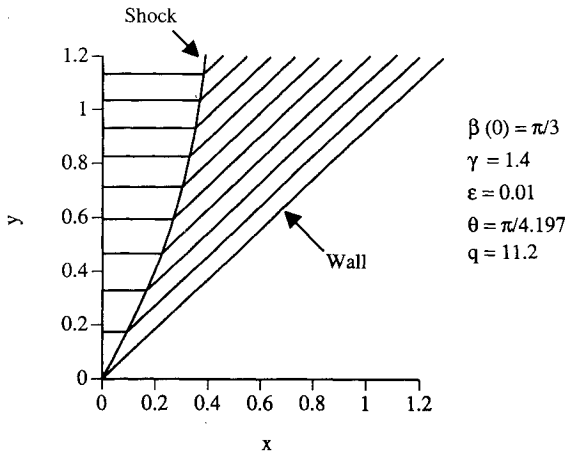

Fig. 6 Shock locus and streamlines for rotational straight-wall curved-shock case.

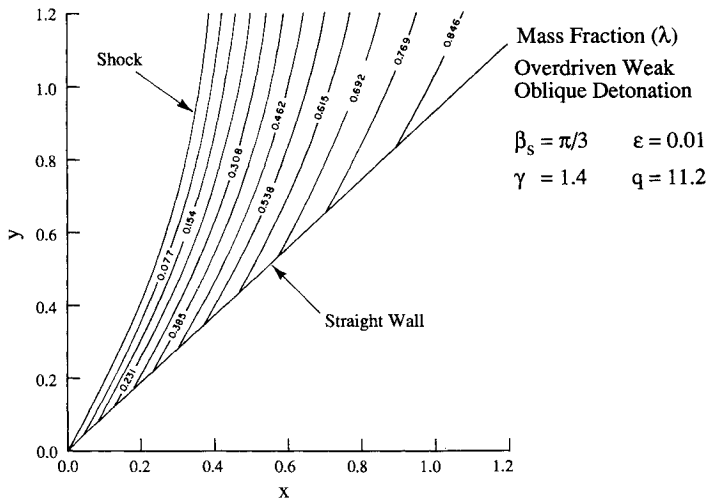

Fig. 7 Reaction product mass fraction field for rotational straight-wall curved-shock case.

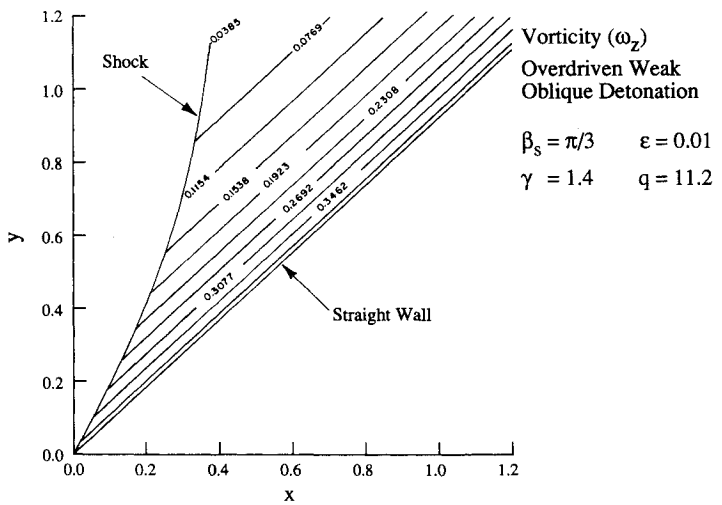

Fig. 8 Vorticity field for rotational straight-wall curved-shock case.

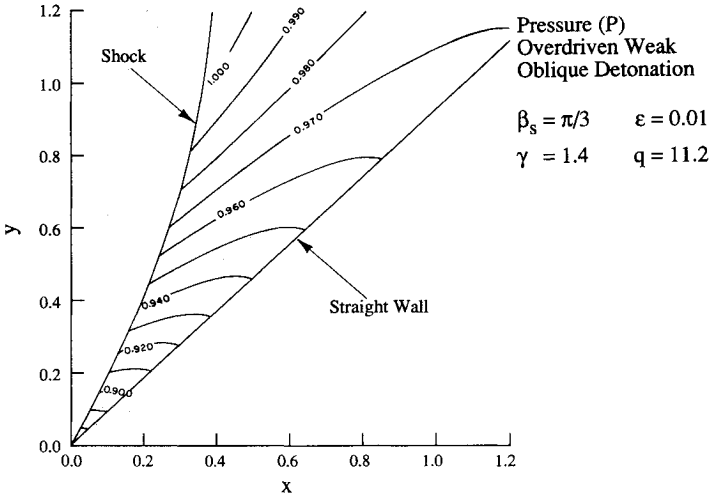

Fig. 9 Pressure field for rotational straight-wall curved-shock case.

numerically integrating the streamline equation. [To return to physical space, one must first use Eq. (12) to translate the shock position and then systematically use the definitions of ξ, ζ, and η to write equations in terms of x and y. In practice, it is easier to generate solutions in ζ-η space and associate each ζ-η point with a point in x-y space.] For each streamline, the shock position is used as the initial condition. On the scales shown in Fig. 6, the streamlines appear to be straight lines parallel to the wedge. In actuality, except for the streamline that passes through the origin, all streamlines have curvature.

There is a continuous variation of the shape of the streamlines depending on their point of origin on the shock. The streamlines are most flat and nearly parallel to the wedge near the wedge in the region with maximum vorticity. As one travels up the shock, streamline curvature increases and shock curvature decreases. Consequently, the vorticity carried on streamlines diminishes with distance from the wedge tip. For all streamlines, except for the streamline coincident with the wedge tip, the initial angle of the streamline is greater than the wedge angle, but relaxes monotonically to the wedge angle as $\xi \to \infty$. Streamlines farthest from the wedge tip suffer the most deflection from a corresponding inert streamline. Far from the wedge tip, the shock has zero curvature; the angle of shock inclination can be determined from Eq. (24). Streamlines in this region are described by the irrotational analysis described earlier in this article.

Figures 7–9 show contours of reaction progress, vorticity, and pressure (λ, ω_z, and P), respectively, for the conditions of Fig. 6. Figure 7 reflects the fact that reaction progress λ varies only with streamwise position ξ. Figure 8 illustrates the vorticity field ω_z, a function of η only. Figures 7 and 8 illustrate the well-known result that the postshock flow is characterized by a reaction layer parallel to the shock and a vorticity layer parallel to the wedge. In these layers, the flow relaxes to an irrotational equilibrium core flow. Figure 9 shows the pressure field, which is a function of both ξ and η. As η increases, the pressure increases due to the increasing shock angle.

Discussion

In this section, the present and future value of this study are discussed. We believe the present value lies in giving explicit analytic verification of many previously expressed ideas regarding oblique detonations, which, as seen in the following paragraphs, can advance the discussion of oblique detonations. The future value of this study lies in its utility as an analytic benchmark for evaluating numerical schemes designed to describe the interaction of nonequilibrium, multidimensional, compressible, shock-laden flows with solid geometries. Such numerical schemes are necessary for the design of any realistic hypersonic device.

First, for the problem of this article, it is legitimate to describe the flow as both a shock-induced combustion and an oblique detonation. It is clear that exothermic reaction is initiated by the shock and can thus be called shock-induced combustion. Furthermore, it is clear that the reaction influences the shock. In the cases studied in which the flow is supersonic, disturbances due to chemical reaction propagate downstream along spatial characteristics. One family of these characteristics reaches back to influence the shock wave. As such, these waves share with one-dimensional detonations the property that chemical reaction effects propagate downstream to influence the lead shock wave. In this sense, and given the close resemblance to oblique shocks, it is appropriate to call these waves oblique detonations.

Second, a heuristic argument based on one-dimensional ZND theory, which shows that for fixed shock angle and one-step irreversible kinetics there is no solution trajectory from the shocked state to the weak underdriven state, has been presented for excluding waves over wedges with wedge angle less than a CJ wedge angle. However, based on analogs with many cases from one-dimensional theory,[28] we speculate that under special circumstances, such as a kinetic scheme characterized by one exothermic and one endothermic reaction, weak underdriven oblique detonations could exist. It is possible to offer other plausible heuristic arguments to exclude weak underdriven waves. These arguments often appeal to hydrodynamic stability theory as it has been applied to nonreactive systems. However, a rigorous determination of the regimes of hydrodynamic stability of oblique detonation waves has never been performed. Such an analysis would involve perturbing the steady solution in space and time and examining under what conditions the disturbance grows. Only recently was the stability of the plane one-dimensional detonation unambiguously resolved.[29] Thus at present one should use caution in a discussion of the stability of these waves. In this light it is more proper to identify those waves that have been identified, i.e., weak overdriven oblique detonations and strong oblique detonations, as steady solutions rather than stable solutions. In a related stability question, the issue of what boundary conditions are necessary for a well-posed problem has not been addressed. Although it is clear that solutions can be constructed for flowfields that are spatially elliptic (the strong case) and spatially hyperbolic (the overdriven weak case), it is not yet established that these solutions are insensitive to small changes in the boundary conditions.

It is also noted that the steady analysis admits a continuum of solutions for incoming Mach numbers greater than the CJ

Mach number; the CJ conditions provide only a lower bound on the incoming Mach number and do not specify the unique flowfield solution. For steady oblique detonations over a fixed wedge, the flowfield is specified by the wedge geometry, heat release, fluid properties, and incoming flow conditions, and in general is not a CJ flowfield.

Finally, it is suggested that these results be compared to other results. We know of no experimental study that reports hypersonic reaction zone observations. Current published numerical solutions generally employ more complicated kinetic models, include viscous transport, or model real gas effects such as dissociation, all of which make direct comparisons difficult and in some cases meaningless. For example, the calculations that show the greatest promise for comparisons are given by Cambier et al.,[17] cases 2 and 4. These cases model hydrogen-air combustion over a 31- and 26.5-deg wedge at incoming Mach numbers of 3.8 and 5, respectively, for a 60% stoichiometric mixture ratio with reaction zone lengths on the order of centimeters. For their case 2 at $M = 3.8$, near the CJ Mach number of 3.38, an additional 5-deg shock angle deflection, which can be detected in their Fig. 5, is attributed to chemical energy release. For the $M = 5$ case 4, it is difficult to detect any shock deflection. The authors suggest that the effects of dissociation at the higher Mach numbers are balancing the effects of heat release. Because case 2 is too close to the CJ solution for the hypersonic limit to be appropriate, because in case 4 dissociation is likely important, and, additionally, because rough estimates indicate that for hydrogen or hydrocarbon fuels the linear analysis is valid only for much leaner mixtures, even qualitative comparisons are tenuous. A study is underway that will allow direct comparisons of numerical solutions and the approximate solutions of this article.

Acknowledgments

J. M. Powers was supported by the United States Office of Naval Research (ONR) under Contract N00014-86-K-0434 and the Jesse H. Jones Faculty Research Program. Richard S. Miller was the ONR Program Manager. D. S. Stewart was supported by Los Alamos National Laboratories LANL-DOE-9XG83831P1 and the National Center for Supercomputing Applications. Matthew J. Grismer, graduate assistant at Notre Dame, prepared many of the figures. The authors gratefully recognize the helpful discussions with Herman Krier with regard to how this article relates to supersonic ramjet combustion. Both authors also appreciate the efforts of the reviewers, whose suggestions have been adopted throughout the article.

References

[1]Pratt, D. T., Humphrey, J. W., and Glenn, D. E., "Morphology of a Standing Oblique Detonation Wave," AIAA Paper 87-1785, June 1987.

[2]Siestrunck, R., Fabri, J., and Le Grives, E., "Some Properties of Stationary Detonation Waves," *Proceedings of the Fourth Symposium (International) on Combustion*, Williams and Wilkins, Baltimore, MD, 1953, pp. 498–501.

[3]Moore, F. K., and Gibson, W. E., "Propagation of Weak Disturbances in a Gas Subject to Relaxation Effects," *Journal of the Aero/Space Sciences*, Vol. 27, No. 2, 1960, pp. 117–127.

[4]Clarke, J. F., "The Linearized Flow of a Dissociating Gas," *Journal of Fluid Mechanics*, Vol. 7, Pt. 4, 1960, pp. 577–595.

[5]Sedney, R., "Some Aspects of Nonequilibrium Flows," *Journal of the Aero/Space Sciences*, Vol. 28, No. 3, 1961, pp. 189–196.

[6]Spence, D. A., "Unsteady Shock Propagation in a Relaxing Gas," *Proceedings of the Royal Society of London, Series A: Mathematical and Physical Sciences*, Vol. 264, No. 1317, 1961, pp. 221–234.

[7]Vincenti, W. G., "Linearized Flow Over a Wedge in a Nonequilibrium Oncoming Stream," *Journal de Mecanique*, Vol. 1, No. 2, 1962, pp. 193–212.

[8]Capiaux, R., and Washington, M., "Nonequilibrium Flow Past a Wedge," *AIAA Journal*, Vol. 1, No. 3, 1963, pp. 650–660.

[9]Gross, R. A., "Oblique Detonation Waves," *AIAA Journal*, Vol. 1, No. 5, 1963, pp. 1225–1227.

[10]Sedney, R., and Gerber, N., "Nonequilibrium Flow Over a Cone," *AIAA Journal*, Vol. 1, No. 11, 1963, pp. 2482–2486.

[11]Rubins, P. M., and Rhodes, R. P., "Shock-Induced Combustion with Oblique Shocks: Comparison of Experiment and Kinetic Calculations," *AIAA Journal*, Vol. 1, No. 12, 1963, pp. 2778–2784.

[12]Lee, R. S., "A Unified Analysis of Supersonic Nonequilibrium Flow over a Wedge: I. Vibrational Nonequilibrium," *AIAA Journal*, Vol. 2, No. 4, 1964, pp. 637–646.

[13]Spurk, J. H., Gerber, N., and Sedney, R., "Characteristic Calculations of Flowfields with Chemical Reactions," *AIAA Journal*, Vol. 4, No. 1, 1966, pp. 30–37.

[14]Bogdanoff, D. W., and Brackett, D. C., "A Computational Fluid Dynamics Code for the Investigation of Ramjet-in-Tube Concepts," AIAA Paper 87-1978, June 1987.

[15]Fujiwara, T., Matsuo, A., and Nomoto, H., "A Two-Dimensional Detonation Supported by a Blunt Body or Wedge," AIAA Paper 88-0098, Jan. 1988.

[16]Wang, Y. Y., Fujiwara, T., Aoki, T., Arakawa, H., and Ishiguro, T., "Three-Dimensional Standing Oblique Detonation Wave in a Hypersonic Flow," AIAA Paper 88-0478, Jan. 1988.

[17]Cambier, J.-L., Adelman, H. G., and Menees, G. P., "Numerical Simulations of Oblique Detonations in Supersonic Combustion Chambers," *Journal of Propulsion and Power*, Vol. 5, No. 4, 1989, pp. 482–491.

[18]Cambier, J.-L., Adelman, H. G., and Menees, G. P., "Numerical Simulations of an Oblique Detonation Wave Engine," *Journal of Propulsion and Power*, Vol. 6, No. 3, 1990, pp. 315–323.

[19]Buckmaster, J. D., and Lee, C. J., "Flow Refraction by an Uncoupled Shock and Reaction Front," *AIAA Journal*, Vol. 28, No. 7, 1990, pp. 1310–1312.

[20]Yungster, S., "Numerical Study of Shock-Wave/Boundary Layer Interactions in Premixed Hydrogen-Air Hypersonic Flows," AIAA Paper 91-0413, Jan. 1991.

[21]Yungster, S., Eberhardt, S., and Bruckner, A. P., "Numerical Simulation of Hypervelocity Projectiles in Detonable Gases," *AIAA Journal*, Vol. 29, No. 2, 1991, pp. 187–199.

[22]Pandolfi, M., Arina, R., and Botta, N., "Nonequilibrium Hypersonic Flows over Corners," *AIAA Journal*, Vol. 29, No. 2, 1991, pp. 235–241.

[23]Hertzberg, A., Bruckner, A. P., and Bogdanoff, D. W., "Ram Accelerator: A New Chemical Method for Accelerating Projectiles to Ultrahigh Velocities," *AIAA Journal*, Vol. 26, No. 2, 1988, pp. 195–203.

[24]Anderson, J. D., *Hypersonic and High Temperature Gas Dynamics*, McGraw-Hill, New York, 1989.

[25]Hayes, W. D., and Probstein, R. F., *Hypersonic Flow Theory Volume I Inviscid Flows*, 2nd ed., Academic, New York, 1966.

[26]Fickett, W., "Shock Initiation of Detonation in a Dilute Explosive," *Physics of Fluids*, Vol. 27, No. 1, 1984, pp. 94–105.

[27]Shepherd, J. E., "Oblique Detonation Wave Structure," *Chemical and Physical Processes in Combustion*, 1988 Fall Technical Meeting of the Eastern Section, Clearwater Beach, FL, Combustion Inst., Pittsburgh, PA, Dec. 1988.

[28]Fickett, W., and Davis, W. C., *Detonation*, University of California Press, Berkeley, CA, 1979.

[29]Lee, H., and Stewart, D. S., "Calculations of Linear Detonation Instability," *Journal of Fluid Mechanics*, Vol. 216, 1990, pp. 103–132.